LM-00K059
October 12, 2000

The Influence of Dissolved Hydrogen on Nickel Alloy SCC: A Window to Fundamental Insight

D.S. Morton, S.A. Attanasio, G.A. Young, P.L. Andresen, T.M. Angeliu

THE INFLUENCE OF DISSOLVED HYDROGEN ON NICKEL ALLOY SCC: A WINDOW TO FUNDAMENTAL INSIGHT

D.S. Morton, S.A. Attanasio, G.A. Young
Lockheed Martin
P.O. Box 1072
Schenectady, NY 12301

P.L. Andresen, T.M. Angeliu
General Electric Corp R&D
1 River Road
Schenectady, NY 12065

ABSTRACT

Prior stress corrosion crack growth rate (SCCGR) testing of nickel alloys as a function of the aqueous hydrogen concentration (*i.e.*, the concentration of hydrogen dissolved in the water) has identified different functionalities at 338 and 360°C. These SCCGR dependencies have been uniquely explained in terms of the stability of nickel oxide. The present work evaluates whether the influence of aqueous hydrogen concentration on SCCGR is fundamentally due to effects on hydrogen absorption and/or corrosion kinetics. Hydrogen permeation tests were conducted to measure hydrogen pickup in and transport through the metal. Repassivation tests were performed in an attempt to quantify the corrosion kinetics. The aqueous hydrogen concentration dependency of these fundamental parameters (hydrogen permeation, repassivation) has been used to qualitatively evaluate the film-rupture/oxidation (FRO) and hydrogen assisted cracking (HAC) SCC mechanisms. This paper discusses the conditions that must be imposed upon these mechanisms to describe the known nickel alloy SCCGR aqueous hydrogen concentration functionality. Specifically, the buildup of hydrogen within Alloy 600 (measured through permeability) does not exhibit the same functionality as SCC with respect to the aqueous hydrogen concentration. This result implies that if HAC is the dominant SCC mechanism, then corrosion at isolated active path regions (*i.e.*, surface initiation sites or cracks) must be the source of localized elevated detrimental hydrogen. Repassivation tests showed little temperature sensitivity over the range of 204 to 360°C. This result implies that for either the FRO or the HAC mechanism, corrosion processes (*e.g.*, at a crack tip, in the crack wake, or on surfaces external to the crack) cannot by themselves explain the strong temperature dependence of nickel alloy SCC.

INTRODUCTION

Several mechanisms, including film-rupture/oxidation (FRO), hydrogen-assisted cracking (HAC), internal oxidation, vacancy condensation and creep-assisted grain boundary rupture, have been proposed to describe the low electrochemical potential stress corrosion cracking (LPSCC) of nickel based alloys in high purity hydrogenated water at elevated temperatures (*i.e.*, 250-360°C). The primary objective of the present work is to evaluate the ability of the FRO and HAC mechanisms to account for the unique SCC dependency upon aqueous hydrogen concentration. A maximum in LPSCC susceptibility has been identified in proximity to the nickel (Ni)/nickel oxide (NiO) phase transition at 360 to 400°C (Figure 1), by SCC growth rate testing[1] and SCC initiation testing[2] performed as a function of the aqueous hydrogen concentration. This effect of aqueous hydrogen concentration on LPSCC has been described by the extent that the corrosion potential of the alloy deviates from the corrosion potential of the Ni/NiO phase transition[1,2]. This corrosion potential difference represents the relative stability of SCC-controlling oxides. A maximum in LPSCC susceptibility is observed in a narrow (~100 mV) region near the Ni/NiO phase transition. Increased SCC near an oxide phase transition is often considered a classic sign of a corrosion-controlled SCC mechanism[3]. Since corrosion is responsible for crack advance in the FRO mechanism and is believed to be the main source of detrimental hydrogen in a HAC mechanism, both mechanisms as applied to LPSCC are essentially corrosion-driven mechanisms.(1)

Aqueous hydrogen concentration is expected to directly affect the extent of metal corrosion, since the electrochemical potential (which is strongly affected by the aqueous hydrogen concentration) often affects corrosion. Similarly, the aqueous hydrogen concentration is expected to affect the hydrogen uptake within nickel based alloys. Other FRO and HAC mechanism subprocesses could also be influenced by the aqueous hydrogen concentration (*e.g.*, oxide rupture, crack tip strain rate). However, the effect of aqueous hydrogen concentration on SCC is expected to be characterized primarily by the influence of aqueous hydrogen concentration on corrosion (FRO and HAC mechanisms), and the resulting buildup of detrimental hydrogen within the metal (HAC mechanism). Specifically, if the FRO mechanism is the dominant LPSCC mechanism, then metal corrosion should exhibit a maximum in proximity to the Ni/NiO phase transition (*i.e.*, the same functionality with respect to aqueous hydrogen concentration as exhibited by LPSCC). Similarly, if the HAC mechanism is the dominant LPSCC mechanism, then the buildup of detrimental hydrogen within the material must exhibit an analogous functionality with respect to the aqueous hydrogen concentration as is observed by LPSCC.

Hydrogen permeation and repassivation/corrosion tests have been conducted as a function of temperature and the aqueous hydrogen concentration. Hydrogen permeation measurements, as discussed below, are a means to measure the extent of metal hydrogen accumulation *in-situ* (*i.e.*, to evaluate the HAC mechanism). Repassivation experiments have the objective of measuring the extent of metallic corrosion (*i.e.*, to evaluate the FRO and HAC mechanisms).

---

(1) The assertion that corrosion must be the dominant source of detrimental hydrogen if a HAC mechanism is responsible for LPSCC is supported by prior SCC data.[1,2] If hydrogen dissolved in the water (*i.e.*, aqueous hydrogen) were the dominant source of detrimental hydrogen in the metal, one would expect SCC susceptibility to increase monotonically with the aqueous hydrogen concentration, rather than exhibiting a maximum in SCC susceptibility.

HYDROGEN PERMEATION EXPERIMENTS

If HAC is the dominant LPSCC mechanism, the buildup of *detrimental* hydrogen within nickel based alloys should exhibit a maximum with respect to the aqueous hydrogen concentration in proximity to the Ni/NiO phase transition (*i.e.*, consistent with the SCC behavior). Hydrogen permeation experiments provide a direct *in-situ* measurement of the hydrogen fugacity at the metal/metal oxide interface as a function of environmental parameters (*e.g.*, temperature, aqueous hydrogen concentration) and material properties (*e.g.*, material, heat treatment, surface condition).

The uptake of hydrogen dissolved within metals is driven by an elevated level of hydrogen at the metal/metal oxide interface. As illustrated in Figure 2, this interfacial hydrogen concentration evolves from two sources: (1) hydrogen dissolved within the water ($fH_2^{aqueous}$) and (2) hydrogen generated through corrosion reactions ($fH_2^{corrosion}$)[2]. The diffusion/permeation of hydrogen from this elevated interfacial concentration gives rise to the buildup of hydrogen within metals[3].

As shown in Figure 3, the test specimen is essentially an Alloy 600 thermowell whose outer diameter is exposed to the aqueous environment and inner diameter to a vacuum. Permeation of hydrogen through the metal is measured by monitoring the pressure buildup within the specimen.

Apparatus

Tests were conducted in a recirculating autoclave facility located at the General Electric Corporate Research and Development Center. A complete description of the autoclave facility has been given previously[4]. The test specimen, see Figure 3, is comprised of a 6" length of 1/4" OD Alloy 600 tubing (0.18" ID). The outer diameter of this tubing was turned down to 0.24" in an effort to reduce the permeation distance (*i.e.*, permeation distance of 0.03"). The material composition of the Alloy 600 tubing is provided in Table 1. The reduced diameter Alloy 600 tubing was welded to an Alloy 600 rod (0.25" diameter) of 12" length (4" within the autoclave) which passes through the autoclave via a standard compression fitting. A 50 mil diameter hole was drilled into the Alloy 600 rod to communicate hydrogen buildup to a 10 torr (0.013 atm) pressure transducer (*i.e.*, permeation distance of 0.1"). A vacuum pump was employed to evacuate the inner cavity of the test specimen to ensure that the hydrogen fugacity at the inside diameter of the test specimen (< 0.013 atm) was insignificant relative to the hydrogen fugacity at the metal/metal oxide interface (*i.e.*, to produce a constant diffusional driving force). A test run entailed evacuating the inner cavity of the test specimen to ~0.05 torr by opening the vacuum pump isolation valve, followed by shutting the vacuum pump isolation valve and monitoring the pressure buildup due to hydrogen accumulation up to 10 torr (0.013 atm).

---

[2] fH_2 is the fugacity or partial pressure of hydrogen in atmospheres. The fugacity is related to the hydrogen concentration within a metal in units of ppm ($C_{hydrogen}$) through the metal's solubility constant S. $C_{hydrogen}=S(fH_2)^{1/2}$.

[3] The transport or flux of hydrogen (J) can be expressed through Fick's first law, $J = \frac{DC_{hydrogen}}{d} = \frac{P}{d}\sqrt{f_{H_2}}$.

D is the diffusion coefficient, d is the diffusional thickness and P is the permeability coefficient (where P=DS). Typically, when the transport driving force is expressed in terms of $C_{hydrogen}$ the transport is referred to as 'diffusion'. When the transport driving force is expressed in terms of $(fH_2)^{1/2}$ the transport is referred to as 'permeation'.

Test Environment

The water chemistry for the hydrogen permeation tests was deaerated high purity water with various levels of aqueous hydrogen. The solution was buffered to a room temperature pH of 10.2 to maintain a near neutral autoclave pH at the test temperature. Tests were performed at multiple hydrogen concentrations (between 1 and 125 cc/kg) at temperatures of 204, 260, 338 and 360°C. The desired hydrogen concentrations were obtained by varying the hydrogen overpressure in the feed tank according to Henry's law. A Henry's law coefficient of 5.9 kPa/(cc/kg), the solubility of hydrogen in water at 25°C, was used for the room temperature calculations. Mixed gases of 6% or 28% hydrogen (argon balance) were used to obtain hydrogen levels less than 20 cc/kg. Since the autoclave turnover rate was relatively rapid (approximately every hour), autoclave effluent dissolved gas levels were analogous to feed tank levels. Oxygen levels for all tests were <10 ppb.

PERMEATION RESULTS

Over 150 hydrogen permeation test runs were conducted. Data from a representative hydrogen permeation test run (338°C and 123 cc/kg) are provided in Figure 4. In this test run it took 1.7 hours for the internal volume of the test specimen to accumulate 10 torr of hydrogen pressure. In all permeation test runs, including the Figure 4 run, the buildup of internal hydrogen pressure was linear with time. This linear buildup confirms the expectation that the hydrogen fugacity at the metal/metal oxide interface was far greater than the hydrogen fugacity in the internal cavity of the specimen (*i.e.*, there was a constant diffusional driving force). Linear least squares regression analyses were performed on the pressure versus time data to calculate the hydrogen accumulation rate in torr/hr. Least square regression correlation coefficients were typically better than 0.99.

Measured hydrogen permeation rates at 338°C are presented in Figure 5a, as a function of the aqueous hydrogen concentration. Note that each data point in the nickel oxide regime represents the maximum observed permeation rate for that specific condition, since permeation rates were found to decrease with exposure time for conditions within the NiO regime (see the discussion below). It is inferred from Figure 5a that the global nickel alloy metal hydrogen content will likely increase with increasing aqueous hydrogen concentration, since it is expected that the metal hydrogen uptake rate is proportional to the rate of hydrogen permeation. *This hydrogen buildup rate functionality appears to be inconsistent with the SCC dependency upon aqueous hydrogen concentration (Figure 5b).* Direct support of the HAC mechanism would have been obtained if the hydrogen permeation and SCC aqueous hydrogen concentration dependencies were similar.

It can be postulated that the dependencies of hydrogen permeation and LPSCC upon the aqueous hydrogen concentration may differ because of the non-strained permeation test condition. An imposed strain (or an imposed stress) may affect hydrogen uptake by producing a stress field ahead of a crack tip[4], or by producing corrosion of bare metal at sites of local oxide rupture.

---

[4] For SCC growth, the distribution of detrimental hydrogen within nickel alloys can depend strongly upon the stress field due to the presence of a crack. However, since SCC initiation (with no overwhelming stress field singularity due to a crack) and growth have a similar SCC functionality with respect to the aqueous hydrogen concentration[1,2], the presence of a crack cannot explain the SCC aqueous hydrogen level functionality. Therefore, the lack of a stress field singularity (crack) in the hydrogen permeation tests does not explain the inconsistency between the aqueous hydrogen concentration dependencies of hydrogen permeation and SCC.

Regarding the corrosion issue, it appears that general corrosion did occur in hydrogen permeation runs conducted in the nickel oxide regime (though the corrosion likely did not involve bare metal exposure). Figure 6 illustrates the hydrogen permeation response when moving between the nickel metal and nickel oxide regimes at 338°C (step 1). When the transition was made from 61 cc/kg (nickel metal regime) to 17 cc/kg (nickel oxide regime), the measured permeation rate decreased with time (~1.3x permeation rate reduction from 1.9 to 1.5 torr/hr in approximately two days). This reduction in permeation rate suggests that corrosion was occurring in the nickel oxide regime, leading to corrosion oxide buildup on the outer diameter of the test specimen. These results suggest that the dominant effect of the general corrosion was to increase the effectiveness of the oxide as a barrier, rather than to increase the hydrogen permeation rate due to corrosion-generated hydrogen. Thus, general corrosion on an unstrained surface does not appear to produce enough hydrogen to be a dominant source of hydrogen uptake into the metal.

The oxide which formed at 338°C in the nickel oxide regime was initially an effective barrier to hydrogen permeation in the nickel metal regime. Specifically, as shown in Figure 6 (step 2) when the transition was made to 88 cc/kg (nickel metal regime), the measured permeation rate was 1.4 torr/hr, which was 3.4x lower than the value measured previously at 88 cc/kg prior to entering the nickel oxide regime (4.7 torr/hr). Interestingly, after 10 days exposure in the nickel metal regime, the permeation rate of ~4.7 torr/hr was reattained. This result implies that it was possible to either: (1) fully reduce the barrier oxide film formed in the nickel oxide regime, or (2) alter the oxide in such a way that hydrogen transport through the oxide was greatly facilitated[(5)]. Note that the ability to form an oxide barrier to hydrogen permeation in the nickel oxide regime and to subsequently reduce the barrier upon transition back to the nickel metal regime was repeatable.

Permeation data indicate that the dominant source of hydrogen within nickel alloys, at least for a non-strained specimen, is from the hydrogen dissolved in the water. This point is better illustrated by plotting the permeation rate versus the square root of the *aqueous hydrogen fugacity.* Through Fick's first law of diffusion, $J = \frac{P}{d}\sqrt{f_{H_2}}$, the permeation flux J (which is proportional to the pressure buildup rate) should vary with the square root of the *total hydrogen fugacity.* Therefore, if the corrosion-generated fugacity is insignificant relative to the aqueous hydrogen fugacity, a plot of the pressure buildup rate verses the square root of the *aqueous hydrogen fugacity* would be a linear function. As illustrated in Figure 7, measured permeation rates at 360°C, 338°C, 260°C and 204°C very closely follow this functionality with respect to the aqueous hydrogen fugacity. This result confirms that in the hydrogen permeation studies the contribution of corrosion to the hydrogen fugacity was insignificant relative to the contribution of the aqueous hydrogen fugacity at the metal/metal oxide interface. It is also noted, that the aqueous hydrogen fugacity functionality in Figure 7 confirms the *a priori* permeation test assumption that the measured pressure buildup is indeed due to hydrogen and not to the buildup of any other species.

---

(5) Available evidence suggests that scenario (2) is more likely, since the surfaces of Alloy 600 exposed in the nickel metal regime typically are not oxide free, but rather form a spinel-type oxide. Contact electric resistance data from Ehrnsten and Saario[5] have shown that Alloy 600 exhibits a much lower surface resistance in the nickel metal regime than in the nickel oxide regime. This result was attributed by the authors to the formation of metallic Ni 'stringers' in the oxide, an assertion which is supported by the experimental observations of Airey[6]. It is believed that hydrogen transport would be facilitated if such Ni stringers are present and can form a continuous pathway through the oxide.

The inconsistency between the HAC SCC mechanism requirement that the dominant source of detrimental hydrogen is from corrosion and the observation that corrosion-generated hydrogen was insignificant in the Alloy 600 permeation studies does not disprove the HAC mechanism but rather reduces its likelihood and delineates conditions that must be imposed upon the mechanism. Specifically, isolated active path regions (*i.e.*, surface initiation sites or cracks) must be actively corroding and generating elevated hydrogen fugacities locally. Since the rate of hydrogen transport is relatively rapid at elevated temperatures[6] the role of these HAC SCC mechanism theorized active path corrosion locations would be to fill nearby hydrogen trapping locations. It can be envisioned that hydrogen may rapidly diffuse from these active path corrosion locations and consequentially raise the hydrogen concentration of nearby hydrogen trapping sites which is in turn detrimental to the SCC resistance. Since the density of these active path locations could be small, especially in a non-strained test specimen, it is conceivable that it was not possible to discern their contribution to the total hydrogen fugacity in the permeation tests. This hypothesis is supported by metal hydrogen absorption studies[7,8] which have identified enhanced hydrogen uptake in Alloy 600 strained specimens which have undergone SCC. Interestingly, enhanced metal hydrogen uptake neither correlated with SCC severity or the coolant hydrogen level[8]. Rather, hydrogen uptake correlated with the maximum stress (or strain). The argument of sparse active path locations of high corrosion-generated hydrogen fugacity is somewhat diminished, however, by the observation in the present work that permeation rates actually decrease with time (*i.e.*, hydrogen fugacity decreases with time) in the nickel oxide regime. Although the amount of general corrosion was sufficient to form a continuous oxide film (*i.e.*, a permeation barrier) in the nickel oxide regime, no contribution from corrosion-generated hydrogen was measured.

Using knowledge of the diffusional lengths and surface areas in the hydrogen permeation system (Figure 3 provides specimen dimensions) and application of the ideal gas law, it is possible to calculate hydrogen permeability values from measured hydrogen pressure buildup rates. Figure 8 compares Alloy 600 permeability values determined in this study to those measured previously for other nickel based materials, Alloy 718[9] and Alloy X-750 (note that the X-750 data were generated previously in our laboratory, by other investigators). The results illustrate that these materials have similar hydrogen permeabilities (*i.e.*, within a factor of 2x). The permeability of Alloy 718 was slightly greater (~1.5x) than that of Alloy 600 or X-750. Compositional differences (*e.g.*, 18% Fe in Alloy 718 compared to ~9% Fe in the other alloys) may contribute to this difference. It is also possible that Alloy 600 and X-750 permeation rates were biased slow because of aqueous corrosion oxides. The Alloy 718 testing was performed in gaseous hydrogen.

The thermal activation energy for nickel alloy hydrogen permeability (~13 kcal/mol) is about half to a third of reported SCC thermal activation energies. While this observation does not rule out the possibility that hydrogen transport is a key subprocess in the mechanism of nickel alloy SCC, it does indicate that it is not the sole controlling process in LPSCC. It should also be noted that reported SCC activation energies could be biased high since SCC activation energy testing is generally not performed under constant oxide stability environments[1]. In other words, many prior activation energy determinations have employed a 'blend' of SCC measurements, with some tests conducted in the nickel oxide regime and some tests conducted in the nickel metal regime.

---

[6] The order of magnitude time for Alloy 600 338°C diffusion along a 2 mil grain would be ~ 1 minute. In contrast, the order of magnitude time for Alloy 600 to crack a grain length at 338°C would be 10 days.

REPASSIVATION TESTS

As stated earlier, any viable candidate LPSCC mechanism must be able to explain the known influence of the aqueous hydrogen concentration on LPSCC (Figure 1). Since corrosion is an important subprocess in many candidate LPSCC mechanisms (including the FRO and HAC mechanisms), the goal of the repassivation tests was to determine whether the aqueous hydrogen dependence in Figure 1 is attributable to corrosion effects. It is reasonable to postulate that the aqueous hydrogen dependence might be related to corrosion effects, since aqueous hydrogen may affect the extent of corrosion via its effect on electrochemical potential and oxide film stability.

To evaluate this issue, repassivation tests were conducted at several temperatures, because prior work by Morton *et al.*[1] showed that aqueous hydrogen may have varying effects at different temperatures. A concern from the outset of the repassivation tests was that hydrogen oxidation might interfere with the measurement. Indig and Groot[10] showed that corrosion rates were overestimated by linear polarization tests in a hydrogenated environment due to the contribution of hydrogen oxidation to the measured current. However, there were at least two reasons to believe that these difficulties might be overcome in the present study. Prior work[11] at 288°C appeared to show that viable repassivation measurements could be made in the presence of relatively low levels of aqueous hydrogen (*e.g.*, ~3.8 cc/kg). Also, initial work performed in the present study using platinum suggested that the background current due to hydrogen oxidation might be readily subtracted from the measured repassivation transient, thus leaving the current due to metal corrosion. The issue of hydrogen oxidation will be discussed in more detail below.

Drop-weight repassivation tests were conducted on Alloy 600 wires at 204, 260, 288, 316, 338 and 360°C, with varying concentrations of aqueous hydrogen (0 to 20 cc/kg H_2). Repassivation testing was conducted at the General Electric Corporate Research and Development Center, in a test facility which was described previously[11]. Specimens were polarized 50 mV anodic to the open-circuit potential (ocp) using a platinum wire as a reference electrode, and IR compensation was not utilized. The test environment was 0.65M H_3BO_3 + 3.4 x 10^{-3}M NaOH + 40 ppm NH_3, similar to that used by Angeliu *et al.*[11]. This solution was selected to provide reasonable ionic conductivity (to minimize IR error) and a pH at test temperature similar to that of primary water.

Repassivation Results with Dissolved Hydrogen

Typical data obtained in the present work are shown in Figures 9a (204°C) and 9b (338°C). At both temperatures, the repassivation current increased as the aqueous hydrogen concentration was raised. A similar trend was also found at all other test temperatures. The trend observed in the present work can be interpreted in at least two ways: (1) actual changes in corrosion susceptibility are produced by varying the hydrogen concentration due to its effect on the electrochemical potential, or (2) the measured current is dominated by hydrogen oxidation rather than corrosion.

Efforts were made to account for the background current due to hydrogen oxidation by measuring the current prior to dropping the weight, measuring the current at relatively long times after the

drop, once the wire had fully repassivated, and testing platinum wires at 50 mV above the ocp[7]. The trend shown in Figure 9 was still obtained at all test temperatures, even when an attempt was made to subtract out the background current. In other words, the repassivation current increased as the aqueous hydrogen concentration was increased. This result led to some concern that the measurements were being masked by hydrogen oxidation (*i.e.*, that the current due to hydrogen oxidation was not being fully subtracted from the measured current).

To test the hypothesis that hydrogen oxidation might be dominating the observed repassivation response, an experiment was conducted on a nickel wire (99.64 % purity) in both the nickel oxide and nickel metal stable regimes. The objective of this test was to compare the data from the nickel metal regime (in which only hydrogen oxidation is expected to occur) to the data in the nickel oxide regime (in which both corrosion and hydrogen oxidation are expected to occur). If hydrogen oxidation is the dominant source of repassivation current, the measured current in the nickel metal regime should be greater than the measured current in the nickel oxide regime.

The nickel wire repassivation tests were conducted at 204°C under two conditions:
(1) 14 cc/kg H_2, polarized 25 mV anodic to the open circuit potential (nickel metal regime), and
(2) 1 cc/kg H_2, polarized 25 mV anodic to the open circuit potential (nickel oxide regime).
The expected corrosion response was verified as shown in Figure 10. The wire tested in the nickel metal regime was essentially oxide free and the wire tested in the nickel oxide regime developed an oxide film. The measured current-time transients are shown in Figure 11. The specimen tested in the nickel metal regime showed higher repassivation currents than the specimen tested in the nickel oxide regime, except at very short times. The total integrated charge during the 10,000 second test was approximately 11.8 C/cm^2 for the specimen in the nickel metal regime and 5.5 C/cm^2 for the specimen in the nickel oxide regime. Although this comparison is imperfect because the hydrogen levels are not identical (and thus the amount of hydrogen oxidation in each test is not identical), the results suggest that the current response is dominated by hydrogen oxidation rather than by corrosion. Therefore, the effort to measure the extent of corrosion of Alloy 600 in repassivation tests with added aqueous hydrogen was unsuccessful, and is unlikely to be improved by any effort to subtract out the background current due to hydrogen oxidation. It appears that non-electrochemical techniques must be utilized in an attempt to elucidate the effect of aqueous hydrogen concentration on the extent of corrosion.

The present results are consistent with some prior repassivation tests[12], in which the addition of hydrogen led to increased currents (attributed to increased hydrogen oxidation). However, the present results are inconsistent with the results of other prior tests,[11,2] in which the extent of corrosion appeared to decrease as the aqueous hydrogen content was increased. This apparent inconsistency in the repassivation response as aqueous hydrogen is added lends further support to the view advanced above -- in other words, it may be more appropriate to use non-electrochemical methods to understand the effect of aqueous hydrogen concentration on the extent of corrosion.

---

[7] Hydrogen oxidation current densities were measured at +50 mV relative to the ocp, both prior to and after the straining of the test specimen. These measurements provided a nearly equivalent background current density (presumably due to hydrogen oxidation) which was subtracted from the measured "repassivation" current density transients. A similar procedure was employed using unstrained platinum wires tested at +50 mV relative to the ocp.

ESCA Corrosion Film Thickness of X-750 as a Function of Dissolved Hydrogen

Electron Spectroscopy Chemical Analysis (ESCA) oxide film thickness determinations were made on external surfaces of three alloy X-750 specimens oxidized under identical conditions (360°C for 28 days) except for the coolant hydrogen level (nitrogen deaerated, 14 and 107 cc/kg). This ESCA analytical investigation was conducted in an effort to non-electrochemically evaluate whether the SCC hydrogen dependence shown in Figure 1 is attributable to corrosion effects. The compact tension specimens whose SCC performance is presented in Figure 1 were employed as the actual ESCA samples. Additional specimen exposure test details are provided in Reference (1). As illustrated in Figure 12, ESCA average oxide film thickness did not exhibit the same functionality that was observed with SCC with respect to the coolant hydrogen level. That is, X-750 HTH 360°C SCC crack growth is ~20 times slower under nitrogen sparge test conditions compared to 14 cc/kg test conditions. However, the nitrogen sparge oxide film thickness was approximately twice as thick as the 14 cc/kg oxide film (6500 compared to 2820 angstroms). Even though a large oxide film thickness uncertainty exists (at least 20% and maybe as high as 50%), this data indicates that SCC and bulk corrosion have different coolant hydrogen level dependencies. These findings are contrary to the Soustelle *et al.*[13] study which found a correlation between bulk oxide film thickness and the extent of SCC.

The lack of correlation between SCC and bulk oxide film thickness suggests that either: 1) bulk surface corrosion is not an accurate measure of the corrosion kinetics that occurs at the crack tip or 2) the functionality of SCC with respect to the coolant hydrogen level is unrelated to a corrosion functionality. The authors view the former argument as being more likely. Steady state bulk surface corrosion kinetics are typically a function of the square root of time due to a process controlled by diffusion through the protective oxide. In contrast, at a crack tip where periodic rupture can occur due to strain accumulation, the kinetics of initial film formation from a bare metal surface are likely controlling the corrosion. The observation of different corrosion product oxide films at the crack tip and upon bulk surfaces of nickel alloys, additionally, supports the first hypothesis.

Nitrogen-Deaerated Repassivation Results

It is believed that reliable repassivation tests can be conducted by deaerating the environment with nitrogen, since such an environment will contain a very low level of aqueous hydrogen[(8)].

This assertion is supported by the qualitative agreement between repassivation tests reported by Attanasio *et al.*[14] (in a nitrogen deaerated environment) and corrosion coupon data obtained by Soustelle *et al.*[13]. The repassivation results[13] implied that Alloy 600 corrodes at a higher rate than Alloy 690, which is qualitatively consistent with the fact that the corrosion film on Alloy 600 was thicker than the film on Alloy 690[14]. The agreement between repassivation data collected in a non-hydrogenated system and actual corrosion has also been shown by Ford and Andresen[15,16]. Increasing the Cr content of Fe-xCr-9.5Ni from 0 to 18% produced a marked decrease in the repassivation current, consistent with the known effect of Cr on the corrosion of stainless steel.

[(8)] Prior data[11] indicate that the aqueous hydrogen concentration in a nitrogen deaerated environment is ~ 0.04 cc/kg.

In the present study, nitrogen deaerated data were collected at 204 to 360°C, as shown in Figure 13. Although some scatter is evident, it is significant that there is little systematic effect of temperature on the corrosion of Alloy 600. This result is qualitatively consistent with limited corrosion coupon data from Copson and Berry[17], where the descaled weight loss after 2000 hours in primary water was similar at 288°C (8-12 mg/dm^2) and 360°C (10-14 mg/dm^2). The present data, along with the prior corrosion coupon data[17], suggest that the corrosion of Alloy 600 in primary water is not strongly activated by temperature. This result implies that corrosion processes occurring at an SCC crack tip, in the crack wake, or on surfaces external to the crack cannot by themselves explain the strong temperature dependence of LPSCC. It is still certainly possible that corrosion contributes to LPSCC (*e.g.*, by direct crack advance as postulated in the FRO mechanism or by facilitating the production of detrimental hydrogen as postulated in the HAC mechanism). However, it is evident that the temperature dependence of LPSCC must be provided by other important subprocesses such as (but not limited to) creep or hydrogen diffusion.

CONCLUSIONS

- The validity of the FRO and HAC LPSCC nickel alloy mechanisms was not proven or disproven by test results of this study. Results from this study, however, have identified conditions that must be imposed upon these SCC mechanisms to describe the known nickel alloy SCCGR aqueous hydrogen concentration functionality. Specifically,

  1) The buildup of hydrogen within Alloy 600 (measured through permeability) does not exhibit the same functionality as SCC with respect to the aqueous hydrogen concentration. This result implies that if hydrogen assisted cracking (HAC) is the dominant SCC mechanism, then **isolated** active path regions (*i.e.*, surface initiation sites or cracks) must be actively corroding and must be the dominant source of elevated detrimental hydrogen fugacities. In the hydrogen permeation studies, the hydrogen fugacity produced by general corrosion was insignificant relative to the aqueous hydrogen fugacity even when active corrosion was occurring;

  2) Drop-weight tests performed in a nitrogen deaerated environment showed that the repassivation of Alloy 600 shows little temperature sensitivity from 204 to 360°C. Therefore, corrosion at an SCC crack tip, in the crack wake, or on external surfaces cannot explain the strong temperature dependence of nickel alloy SCC;

  3) The hydrogen permeability thermal activation energy for nickel alloys (~13 kcal/mol) is about half to a third of the reported SCC thermal activation energies. This suggests that hydrogen transport cannot be the sole controlling process for nickel alloy SCC.

- The permeability of Alloy 600 is nearly equivalent to that of other nickel based alloys (*i.e.*, Alloys 718 and X-750). An appreciable hydrogen permeation oxide film barrier did not form upon exposure to environmental conditions in which nickel metal is thermodynamically stable. A significant hydrogen permeation barrier did form upon exposure to conditions in which nickel oxide is thermodynamically stable.

- Repassivation tests could not be effectively performed in environments containing added aqueous hydrogen, due to an apparent interference from hydrogen oxidation. It appears

that non-electrochemical techniques should be used to elucidate the effect of aqueous hydrogen concentration on the extent of corrosion.

- Alloy 600 ESCA bulk surface corrosion film thickness measurements did not exhibit the same functionality as SCC with respect to the coolant hydrogen level. This observation suggests that either:
  (1) bulk surface and crack tip corrosion kinetics are different, or
  (2) the functionality of SCC with respect to the coolant hydrogen level is unrelated to a corrosion functionality.

ACKNOWLEDGEMENTS

The following individuals are recognized for their contribution to this effort:

- Bill Catlin and Mike Pollick for their assistance in test design and for their diligence in test facility operation.
- Carl Grove and Lee Petzold for their pioneering nickel alloy high purity water hydrogen permeation studies.
- Mike Hanson for his alloy X-750 ESCA analyses.

REFERENCES

(1) DS Morton, SA Attanasio, JS Fish and MK Schurman, "Influence of Dissolved Hydrogen on Nickel Alloy SCC in High Temperature Water" Corrosion 1999 NACE Conference, Paper 447, April 1999.
(2) T. Cassagne, B. Fleury, F. Vaillant, O. de Bouvier, P. Combrade, "An Update on the Influence of Hydrogen on the PWSCC of Nickel Base Alloys in High Temperature Water", Proc. of the Eighth International Symposium on Environmental Degradation of Materials in Nuclear Power Systems-Water Reactors, p.307, August 1997.
(3) PM Scott, "An Overview of Internal Oxidation as a Possible Explanation of Intergranular Stress Corrosion Cracking of Alloy 600 in PWRs", Proc. of the Ninth International Symposium on Environmental Degradation of Materials in Nuclear Power Systems-Water Reactors, August 1999.
(4) DS Morton, D. Gladding, MK Schurman, CD Thompson, Proc. of the Eighth International Symposium on Environmental Degradation of Materials in Nuclear Power Systems-Water Reactors, p.387, August 1997.
(5) U. Ehrnsten *et al.*, Fourth EPRI Workshop on PWSCC, Daytona Beach, 1997.
(6) GP Airey, EPRI Report NP-3051, Palo Alto CA, 1983.
(7) N. Totsuka et al., "Effect of Hydrogen on the Intergranular Stress Corrosion Cracking of Alloy 600 in High Temperature Aqueous Environments," *Corrosion*, Vol. 43 1987.
(8) T. Magnin, JM Boursier, D. Noel, R. Rios, and F. Vaillant, "Corrosion Deformation Interaction During Stress Corrosion Cracking of Alloy 600 in Primary Water", Proc. of the Sixth International Symposium on Environmental Degradation of Materials in Nuclear

(9) WM Robertson, "Hydrogen Permeation and Diffusion in Inconel 718 and Incoloy 903," *Metallurgical Transactions*, Vol. 8a, 1977.
(10) ME Indig and C. Groot, "Some Limitations of the Linear Polarization Techniques in Evaluating Corrosion Behavior", *Corrosion*, Vol. 25, No. 11, November 1969.
(11) TM Angeliu, PL Andresen, ML Pollick, "Repassivation and Crack Propagation of Alloy 600 in 288°C Water", Corrosion 1996 NACE Conference, Paper 86, April 1996.
(12) F. Valliant, JD Mithieux, O. de Bouvier, D. Vancon, G. Zacharie, Y. Brechet, and F. Louchet, "Influence of Chromium Content and Microstructure on Creep and PWSCC Resistance of Nickel Base Alloys", Proceedings of the Ninth International Symposium on Environmental Degradation of Materials in Nuclear Power Systems, Newport Beach, CA, 1999.
(13) C. Soustelle, M. Foucault, A. Gelpi, P. Combrade, and T. Magnin, "PWSCC of Alloy 600: A Parametric Study", Proc. of the Ninth International Symposium on the Environmental Degradation of Materials in Nuclear Power Systems, Newport Beach, CA, 1999.
(14) SA Attanasio, JS Fish, WW Wilkening, PM Rosecrans, DS Morton, GS Was, and Y Yi, "Measurement of the Fundamental Parameters for the Film-Rupture/Oxidation Mechanism - The Effect of Chromium", Proc. of the Ninth International Symposium on Environmental Degradation of Materials in Nuclear Power Systems, Newport Beach, CA, 1999.
(15) FP Ford, "The Crack Tip System and its Relevance to the Prediction of Cracking in Aqueous Environments", from Environment-Induced Cracking of Metals (NACE-10), Ed. RP Gangloff and MB Ives, October 1988.
(16) PL Andresen "Conceptual Similarities and Common Predictive Approaches for SCC in High Temperature Water Systems", CORROSION/96, Paper No. 258, 1996.
(17) HR Copson and WE Berry, "Qualification of Inconel for Nuclear Power Plant Applications", *Corrosion*, Vol. 16, (page 79t), 1960.

TABLE 1 - MATERIAL COMPOSITION

Element	Alloy 600 Heat NX8147 (Permeation)	Alloy 600 Heat NX8517G18 (Repassivation)	Nickel Heat N56POAG (Repassivation)
C	0.021	0.06	0.004
Mn	0.20	0.21	0.24
Fe	8.70	8.63	0.04
S	0.001	<0.001	0.001
Si	0.17	0.2	0.02
Cu	0.01	0.09	0.02
Ni	75.22	74.8	99.64
Cr	15.17	15.66	N/A

Figure 1: Nickel Alloy SCC Susceptibility as a Function of Dissolved Hydrogen Concentration

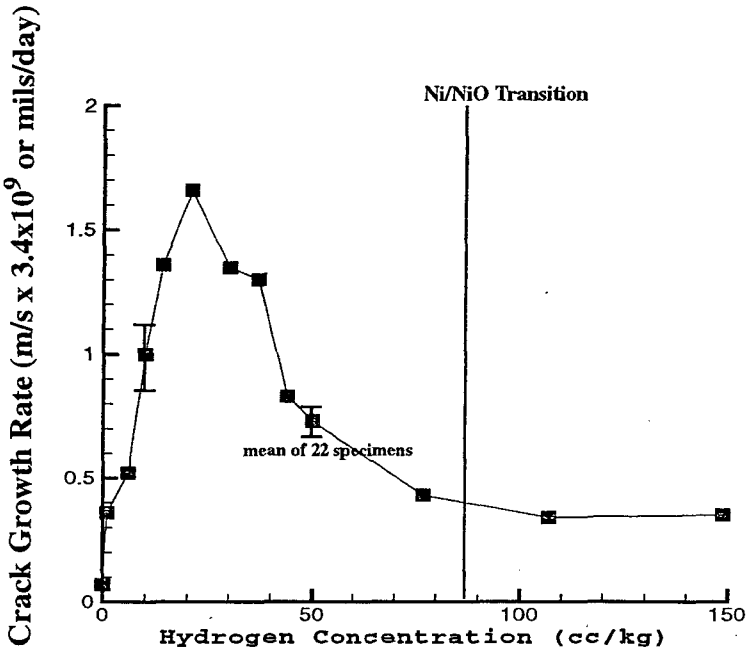

a) X-750 HTH, 360°C, 49 MPa$\sqrt{m}$, crack growth rate vs. H_2 concentration[1]

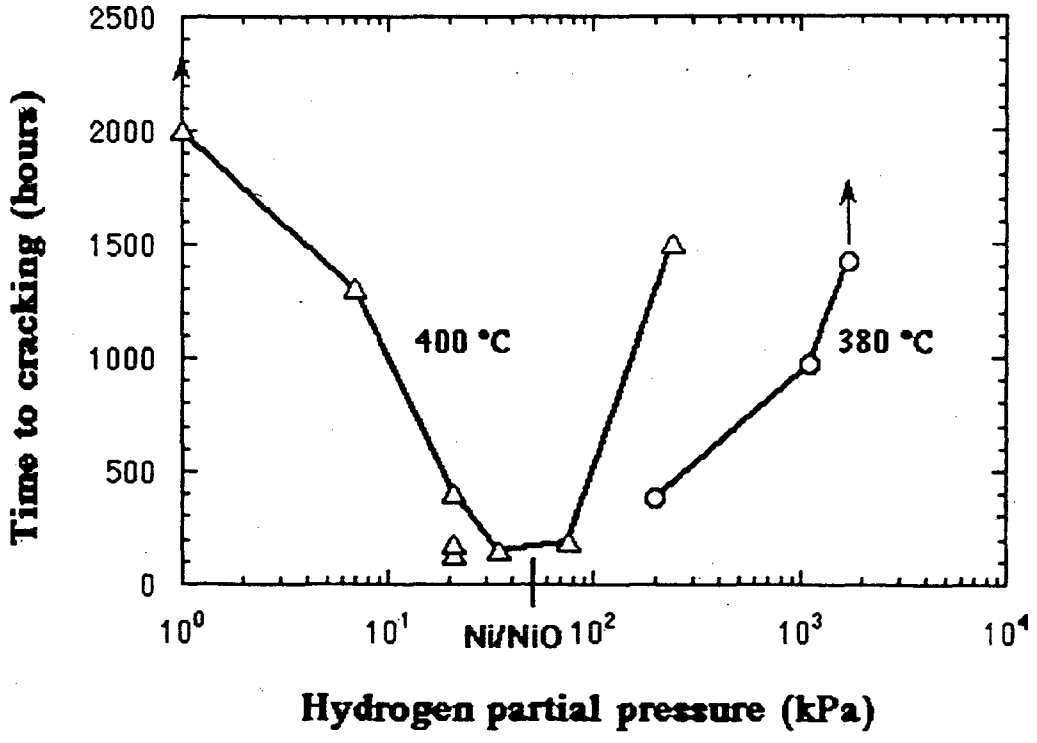

b) Influence of hydrogen on alloy 600 SCC initiation[2]

Figure 2: Total Hydrogen Fugacity at the Metal/Metal-Oxide Interface Drives Metal Hydrogen Uptake and Permeation

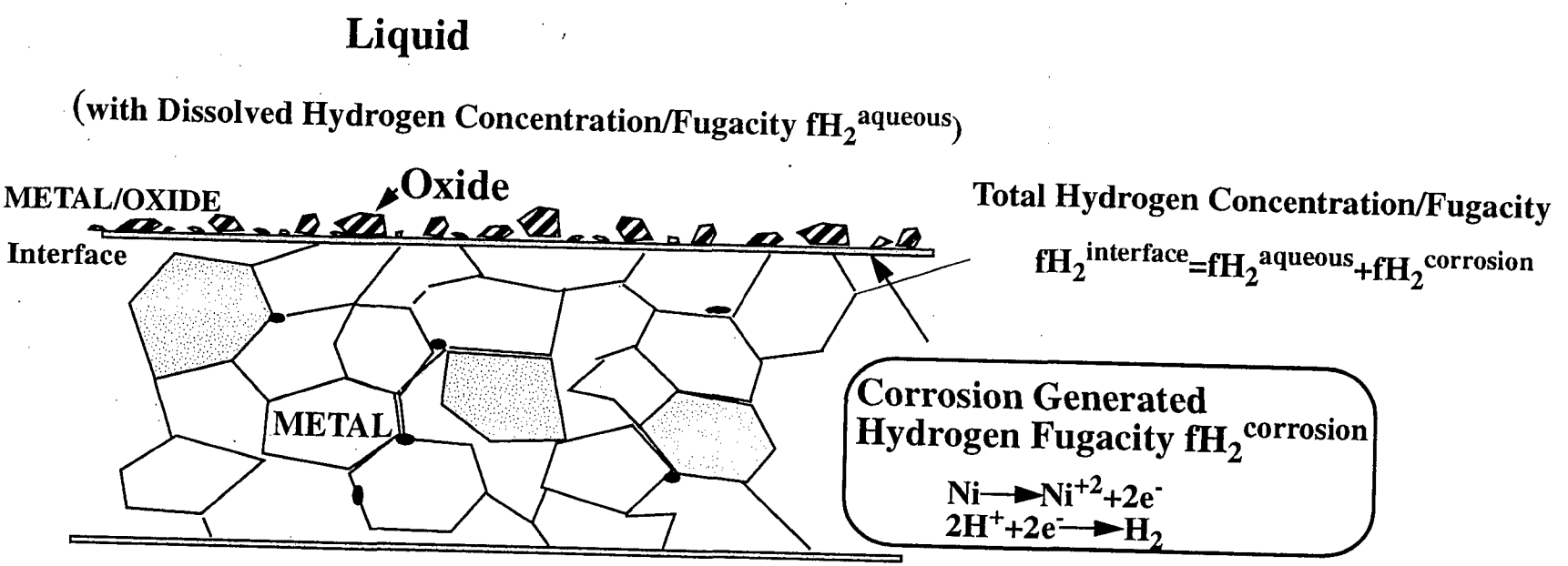

Figure 3: Hydrogen Permeation Test System and Specimen

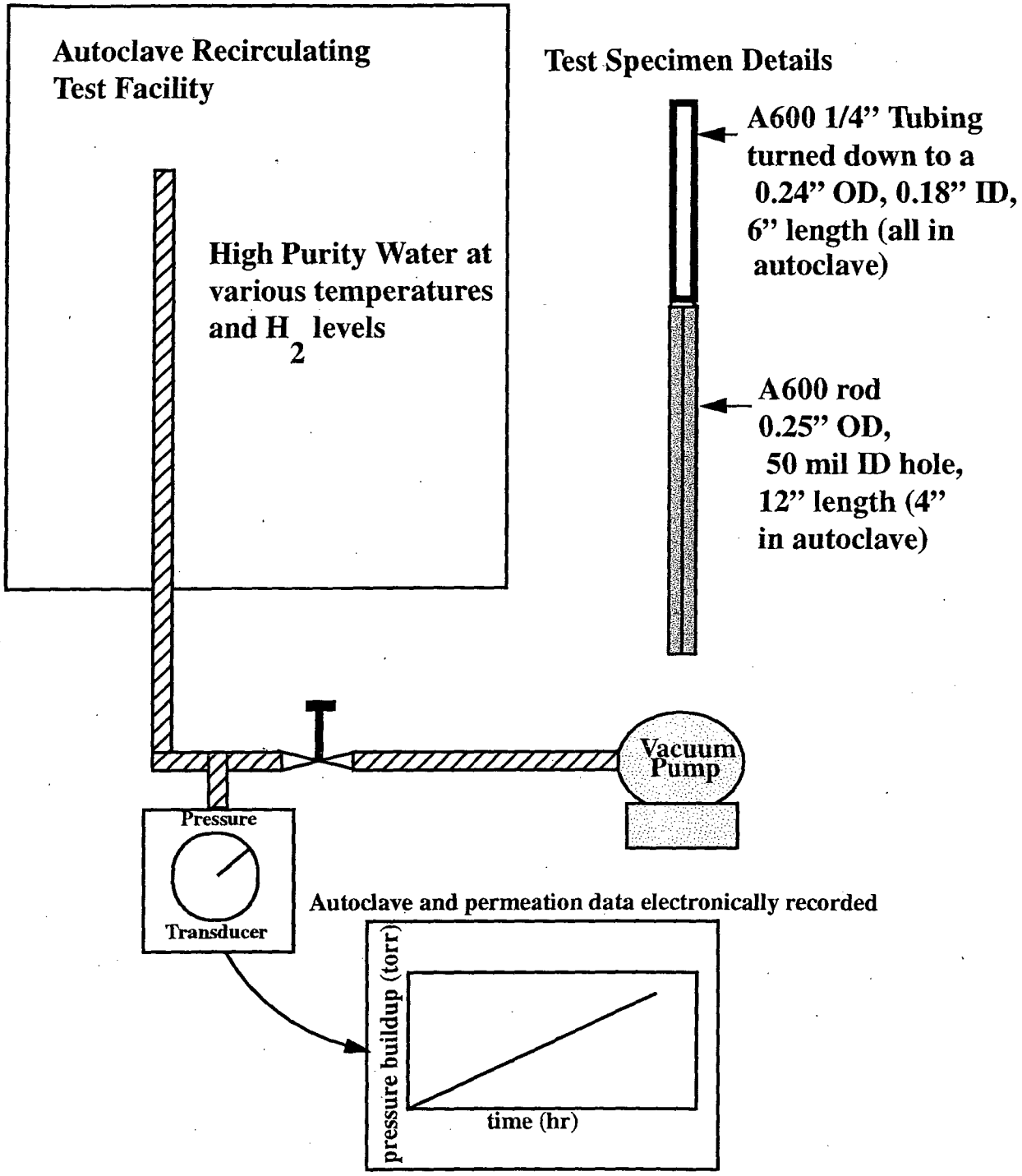

FIGURE 4: Representative Hydrogen Permeation Data (338°C, 123 cc/kg)

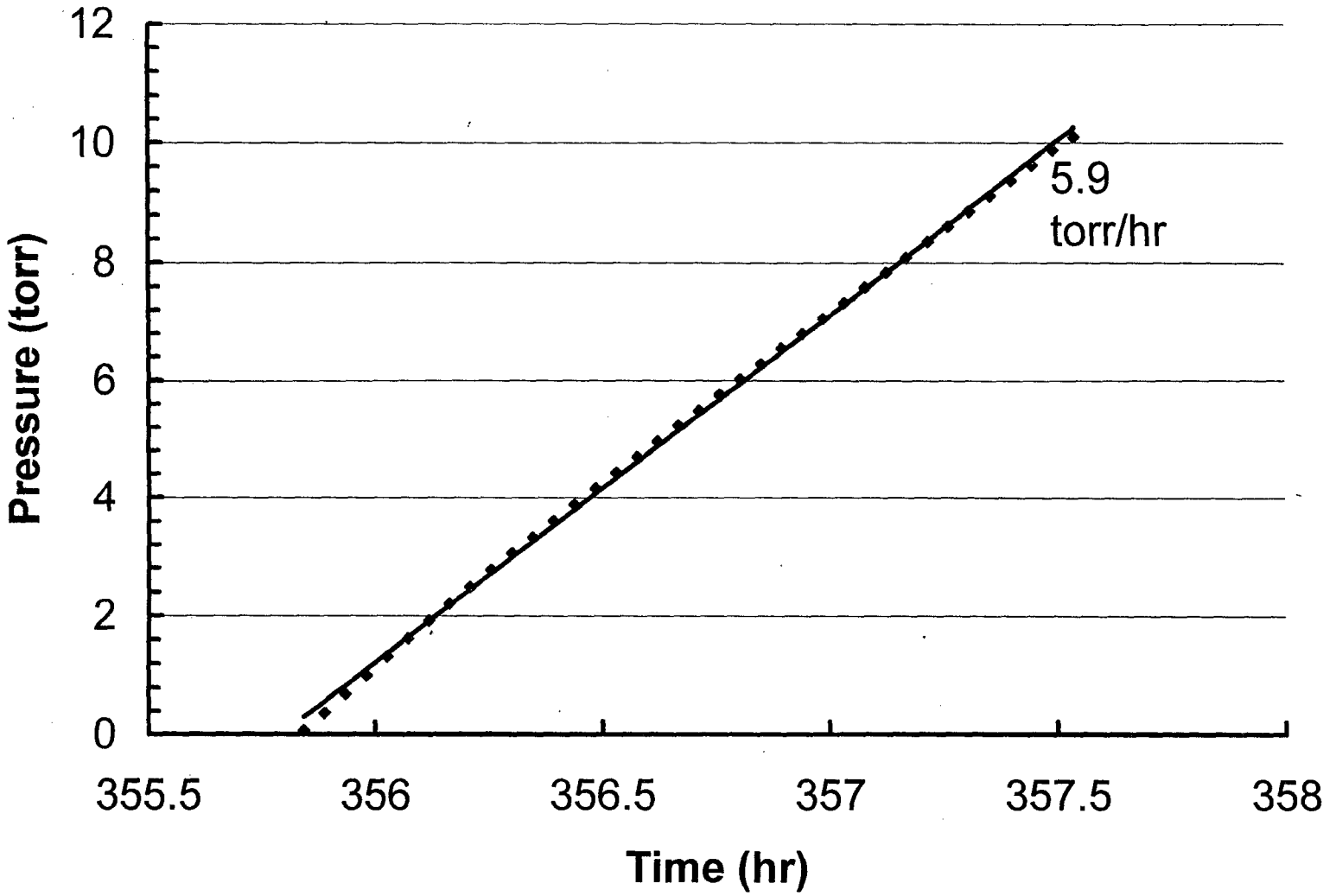

Figure 5: 338°C Hydrogen Buildup and Crack Growth vs. the Aqueous Hydrogen Concentration

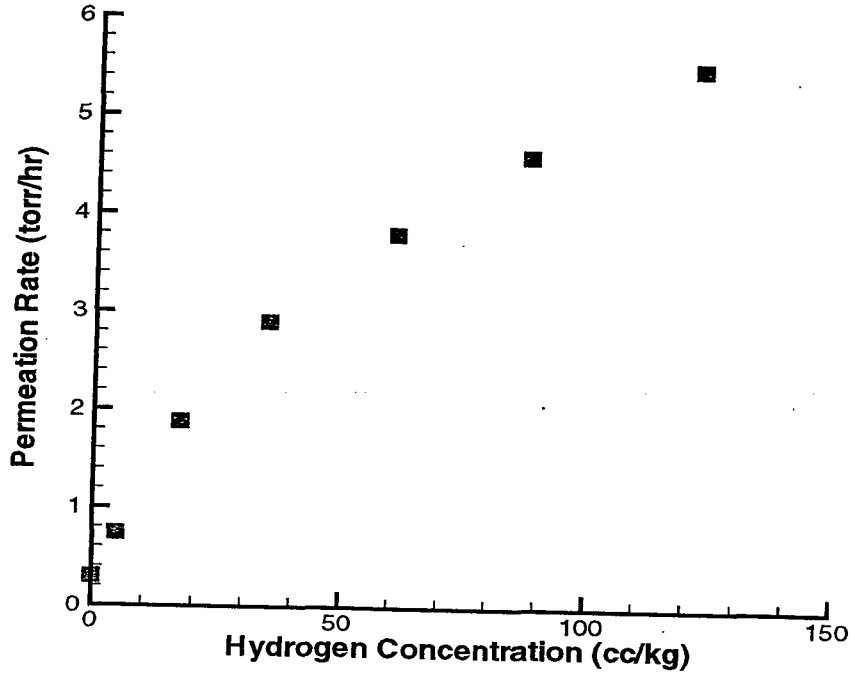

a) Alloy 600 338°C hydrogen buildup vs. hydrogen level (points in the NiO regime are maximum observed rates. Permeation rate decreased with exposure time in the NiO regime)

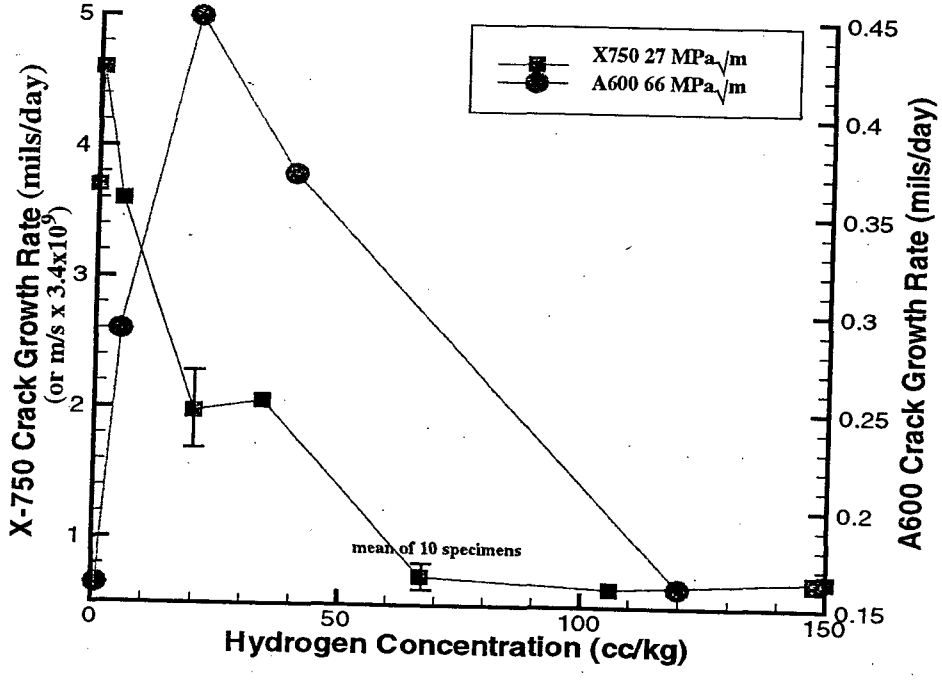

b) Alloy 600 and X-750 338°C crack growth rate vs. hydrogen level[1]

FIGURE 6: 338°C Permeation Data Showing Oxide Film Formation and Reduction

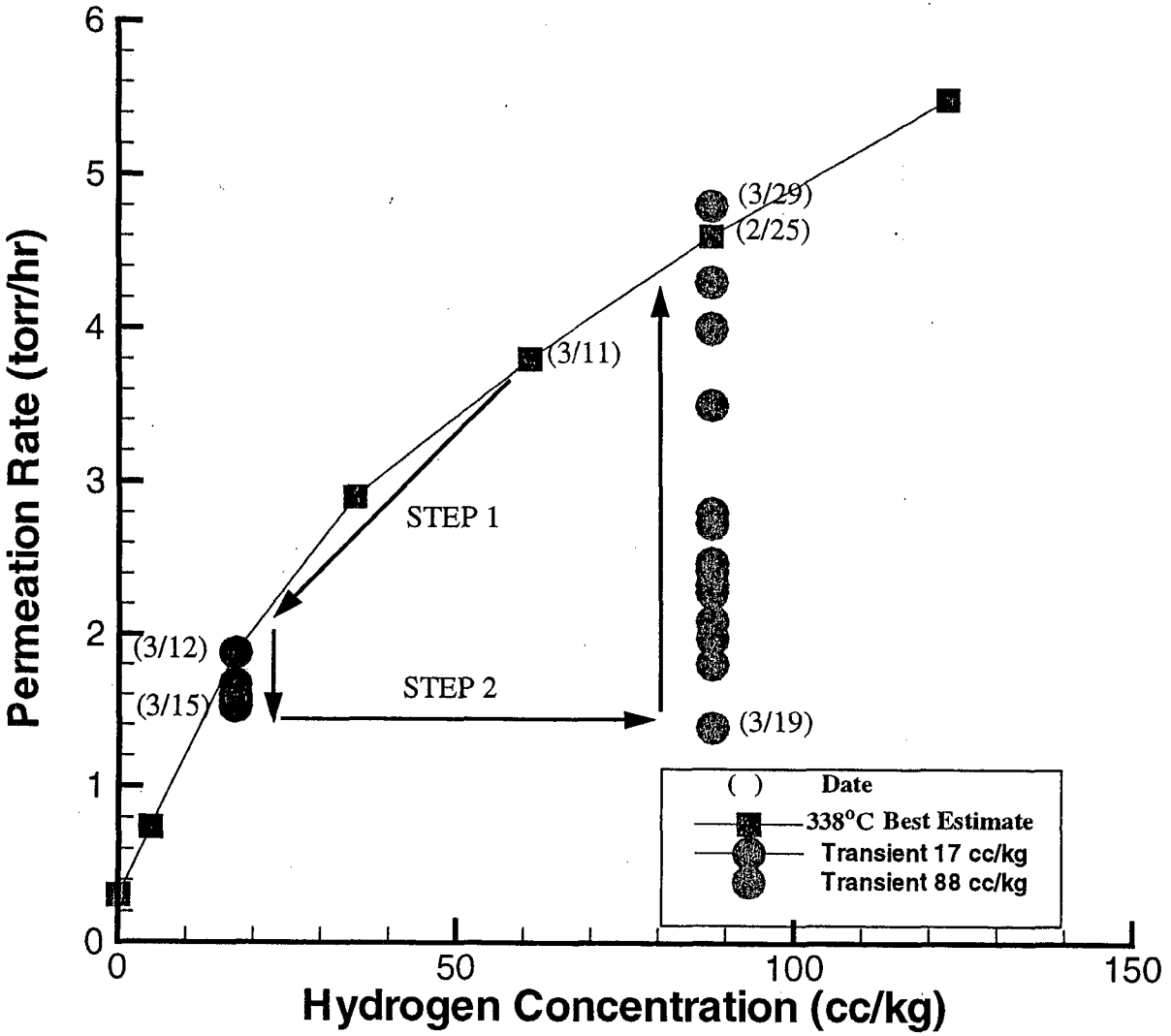

Figure 7: Hydrogen Buildup vs. the Square Root of the Aqueous Hydrogen Fugacity

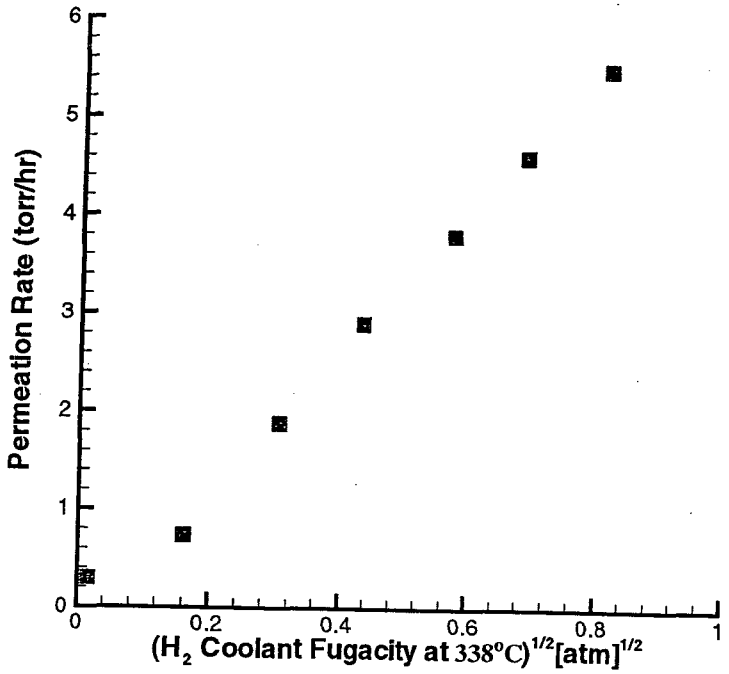

a) Alloy 600 338 °C hydrogen buildup vs. the square root of the aqueous hydrogen fugacity*

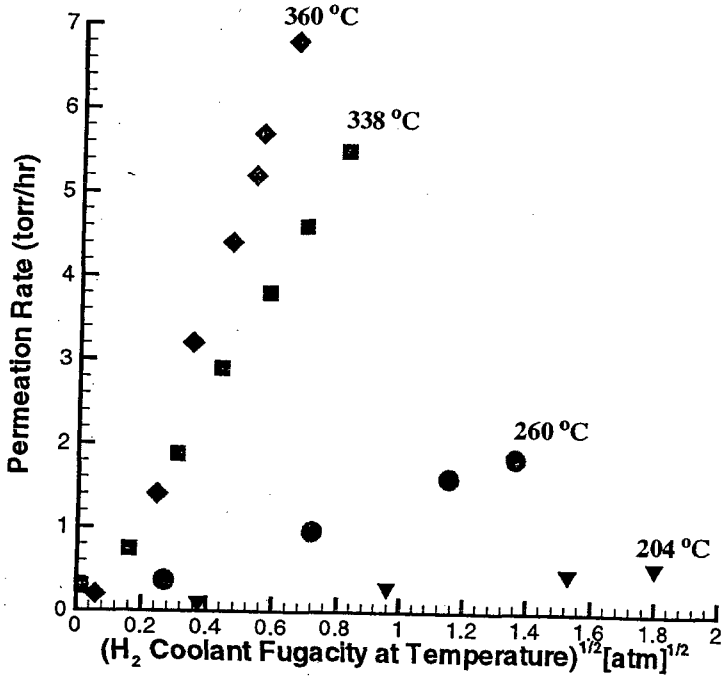

b) Alloy 600 hydrogen buildup vs. the square root of the aqueous hydrogen fugacity*
*(points in the NiO regime are maximum observed rates. Permeation rate decreased with exposure time in the NiO regime)

FIGURE 8: Nickel Based Alloy Hydrogen Permeability vs. Temperature

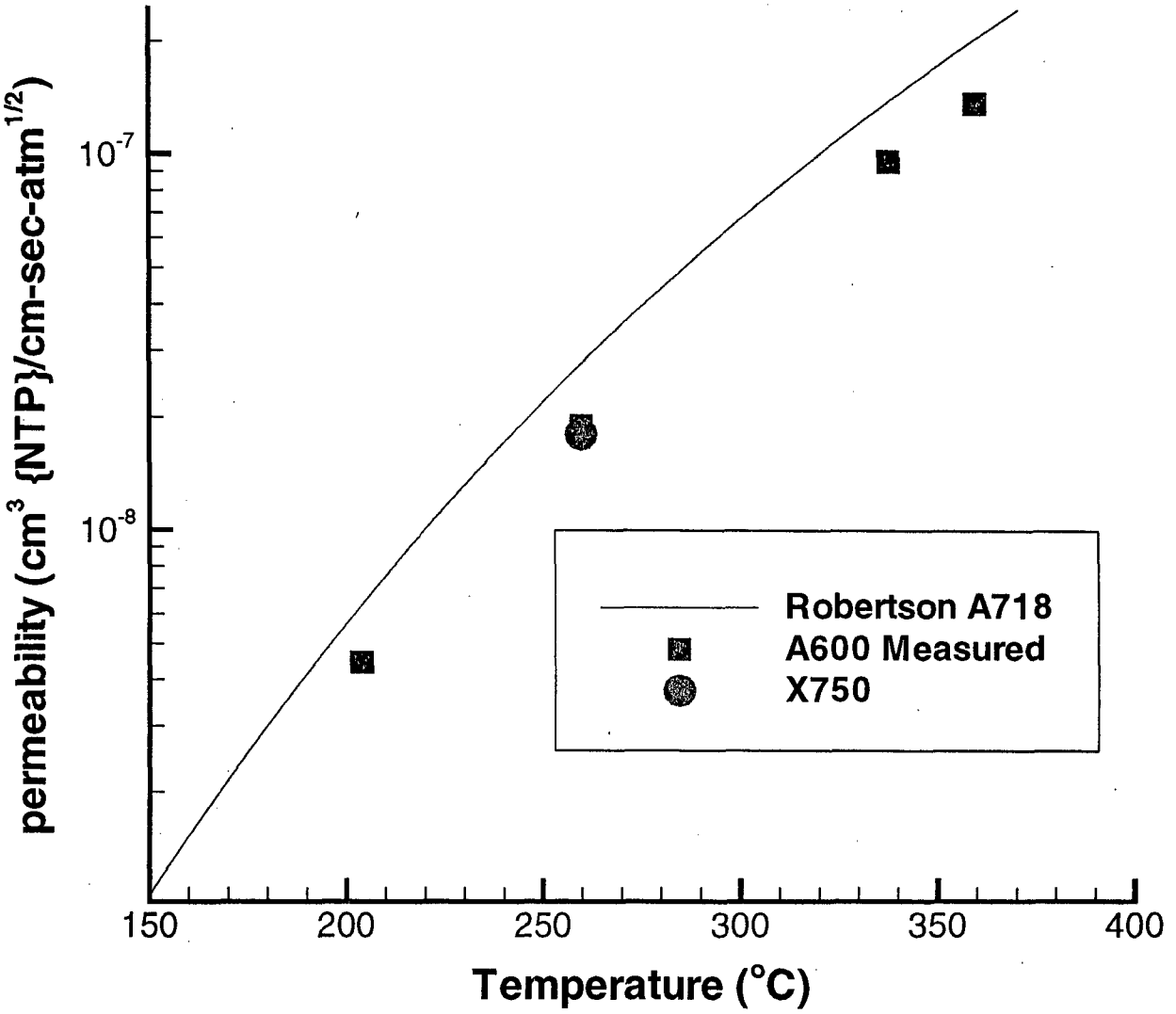

Henry's law coefficients of 0.35, 0.48, 1.5, 2.8 kPa/(cc kg) were employed to convert dissolved hydrogen concentration (i.e., cc/kg) to hydrogen fugacity at temperature for temperatures of 360, 338, 260 and 204°C, respectively.

Figure 9: Alloy 600 Apparent Repassivation Results at 204 and 338°C as a Function of Hydrogen Concentration (cc/kg)

a) 204°C

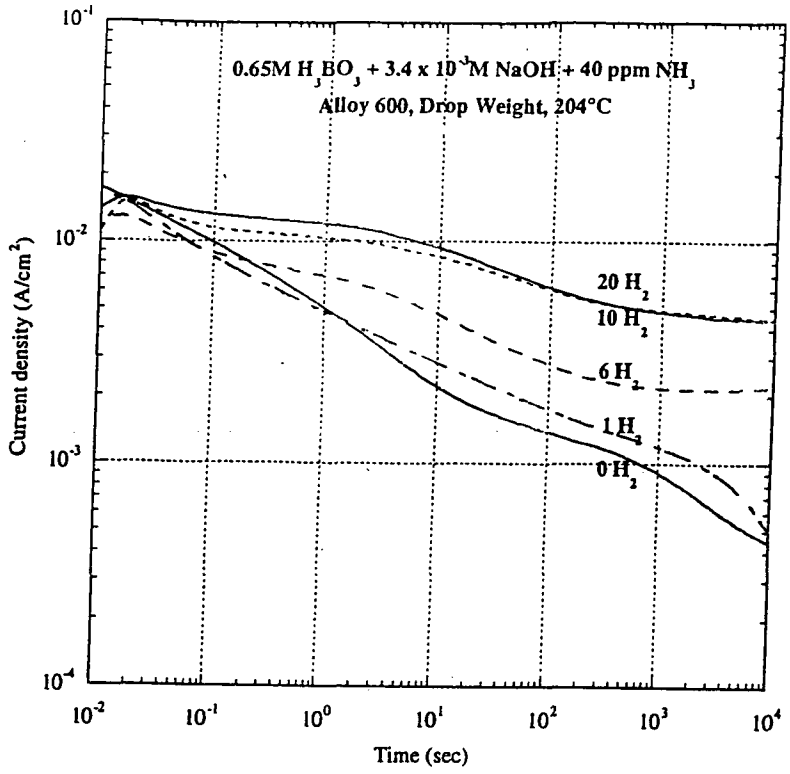

b) 338°C

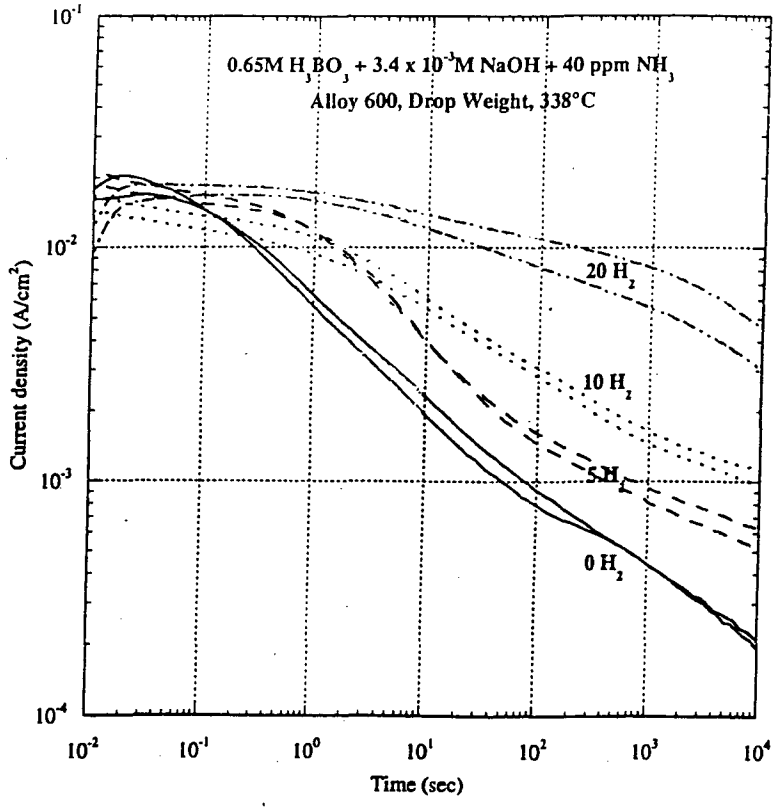

FIGURE 10: Nickel Wire 204°C Repassivation Results

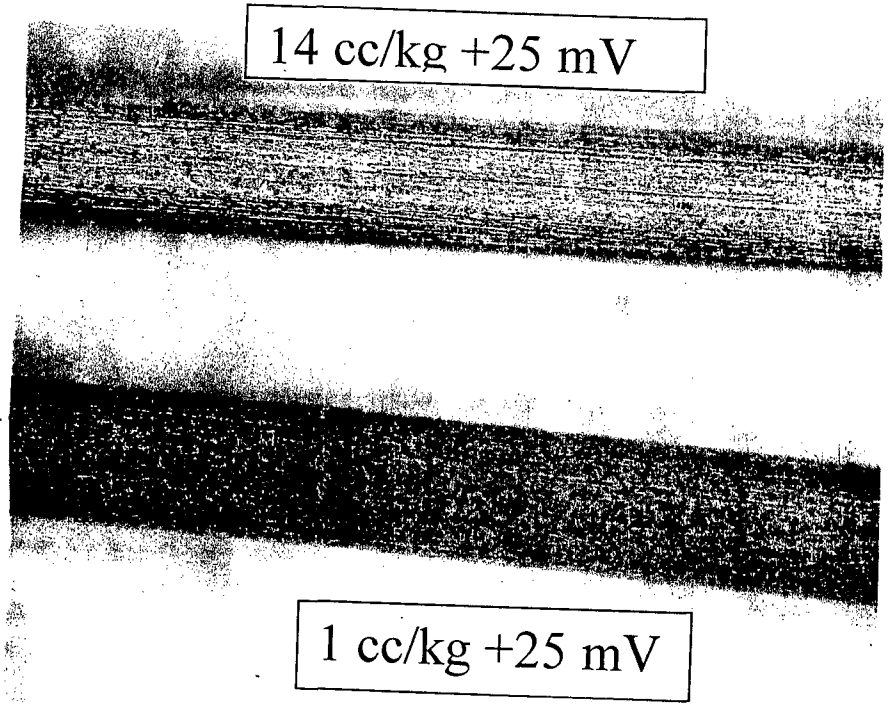

oxide film formation upon nickel oxide environment exposure. Insignificant oxide film formation upon nickel metal regime environment exposure.

Figure 11: Nickel Wire 204 ^{o}C Repassivation Results

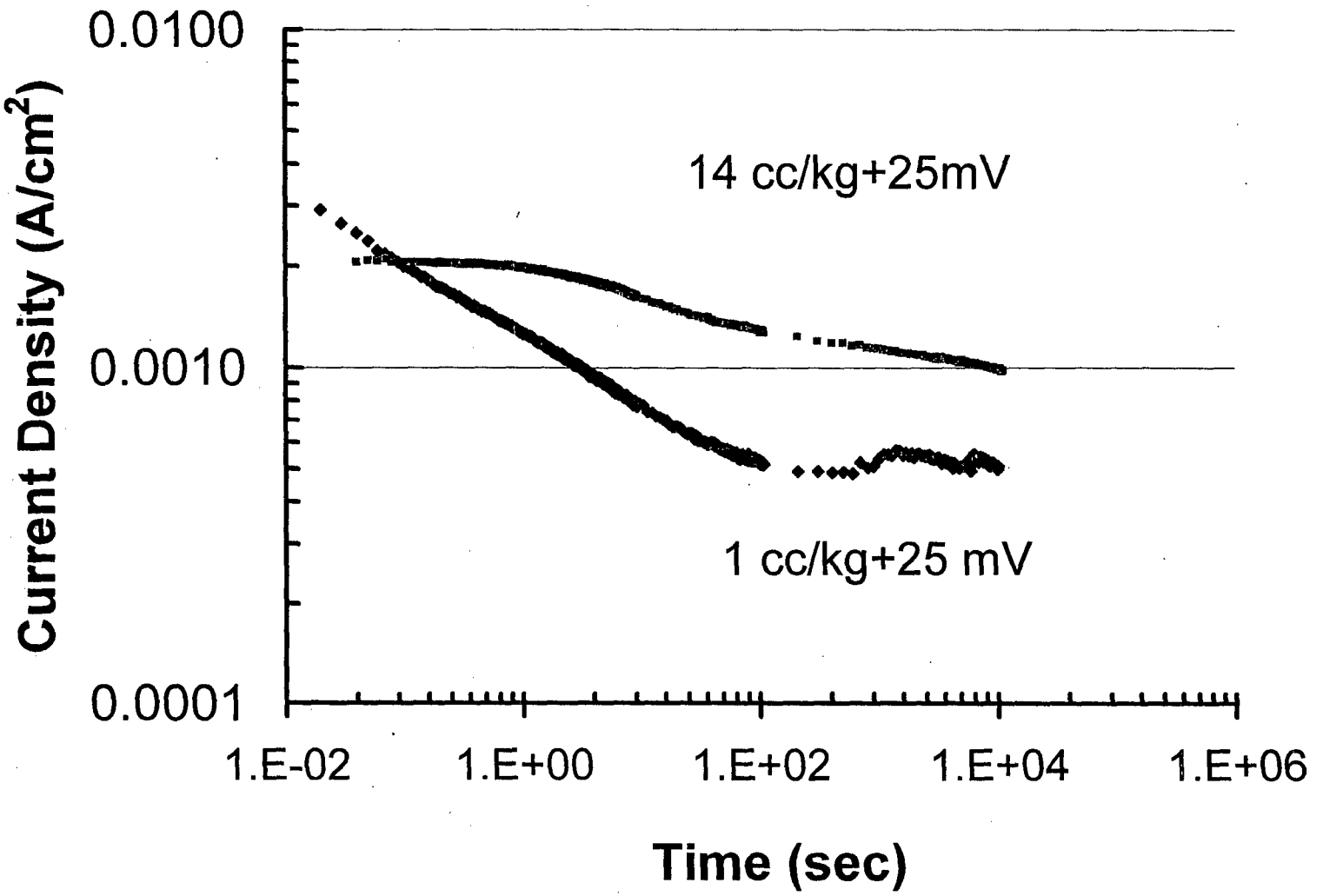

greater current response from specimen tested in 14 cc/kg which did not form an oxide film compared to the specimen which formed an oxide film.

Figure 12: Nickel Alloy SCC and ESCA Oxide Film Thickness as a Function of Dissolved Hydrogen Concentration

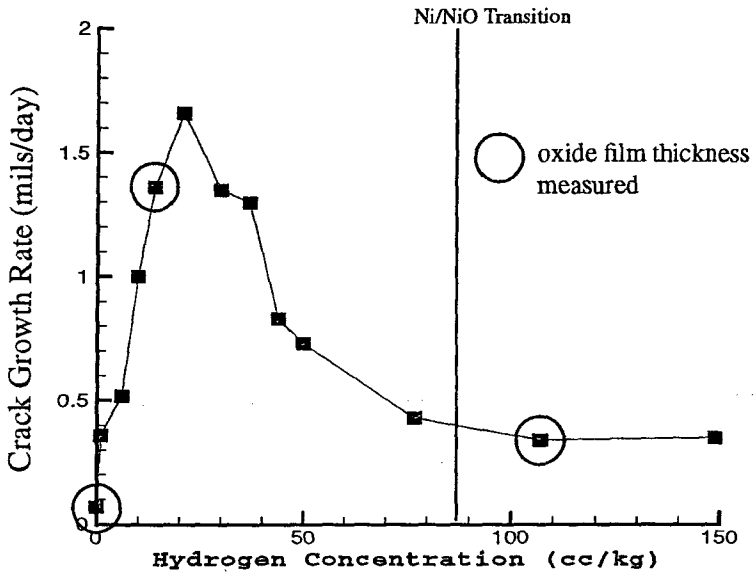

a) X-750 HTH, 360°C, 49 MPa$\sqrt{m}$, crack growth rate vs. H_2 concentration[1]

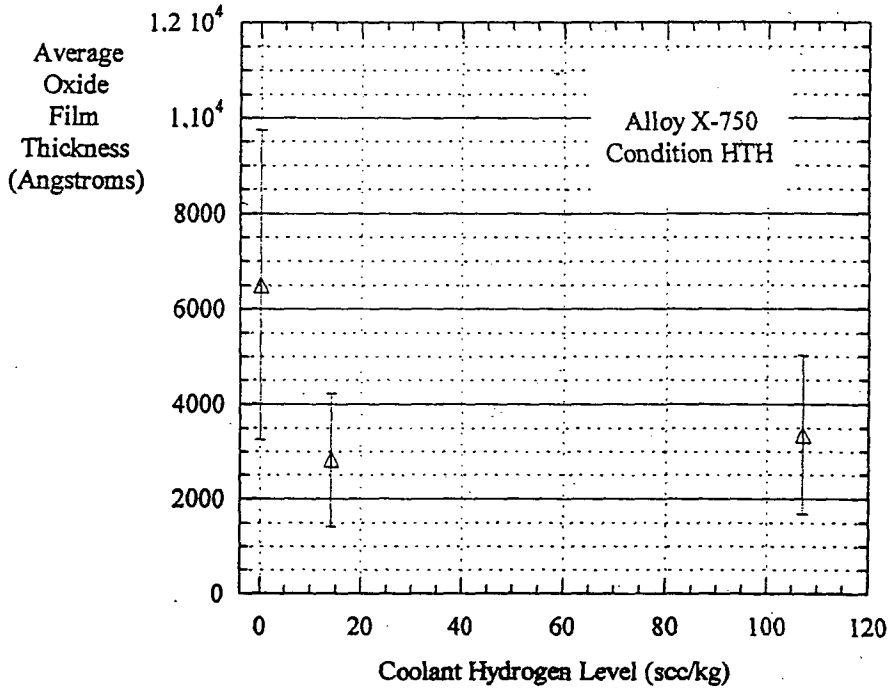

b) X-750 HTH, 360°C, 28 day ESCA determined oxide film thickness vs. H_2 concentration (ESCA measurements were made on the actual CT specimens whose crack growth rates were reported in Figure 12a and highlighted)

FIGURE 13: Repassivation Response as a Function of Temperature (Nitrogen Deaerated)